NON-HERMITIAN QUANTUM MECHANICS: THEORY AND EXPERIMENTS NOT AMENABLE TO CONVENTIONAL QM

EDVARDAS NAREVICIUS AND NIMROD MOISEYEV
Department of Chemistry and Minerva Center of Nonlinear Physics in Complex Systems Technion – Israel Institute of Technology Haifa 32000, Israel

Abstract. Using the conventional QM it is hard and often even impossible to study the dynamics of a system when the two open channels for ionization and molecular dissociation are strongly coupled. The non-Hermitian QM enables us to simplify the problem by introducing a complex adiabatic potential energy surfaces. The complex adiabatic approach enables the separation of the slow and fast motions. The slow/fast motions can be associated with heavy/light particles or with a single particle having very different motion frequencies along the reaction coordinate and the other coordinates. Using the complex adiabatic approach the appearance of narrow peaks in the e^-/H_2 scattering experiments and the sharp phase transition in electron transition through a quantum dot experiments are explained. Possible mechanisms are proposed.

1. Introduction

Recently there is a growing interest in non Hermitian quantum mechanics. Non Hermitian (NH) quantum mechanical (QM) formalism is being used to study and explain physical phenomena. Sharp structures in electron/molecule collision cross sections and abrupt change of the phase of the transition probability amplitude associated with an electron traversing quantum dot are only a few of many examples.

In conventional QM any physically observable quantity is given by the expectation value of a corresponding Hermitian operator. Also the problems studied using the NH-QM can be defined in terms of Hermitian operators only. However this may lead to a system with a very large number

J. Maruani et al. (eds.), Advanced Topics in Theoretical Chemical Physics, 311-338.

of degrees of freedom. For example, consider the dynamics of molecular systems where the electronic and the nuclear coordinates are strongly coupled to one another. In such a case the Born Oppenheimer approach is not applicable and the calculations must involve both nuclear and electronic coordinates. The calculations may be simplified using the non Hermitian quantum mechanics that enables us to take into consideration the coupling between the channels that are open for dissociation and ionization in a simple way [1, 2]. Another example is a dynamical system coupled to a bath. Often the solution of the full problem is impossible due to the current available computational sources and technology. The calculations become possible by including complex absorbing potential terms (i.e., non Hermitian operators) into the Hamiltonian which introduce the environmental dynamical effects on the studied system [3, 4].

2. Non Hermitian adiabatic theory

In this section we will provide the formalism for an extension of the Born-Oppenheimer adiabatic approximation that deals with unstable autoionizing molecules and takes into account the coupling between electronic and nuclear motion. The new formalism will be applied in two cases: (i) full collision process of vibrational excitation of H_2 molecule by electron impact [8], (ii) half collision process of interatomic Coulombic decay of electronically excited Ne cationic dimer [9, 10].

(i) *e/H_2 scattering process*

The most usual method that allows the coupling between electronic and vibrational degrees of freedom of molecule is the Born-Oppenheimer (BO) approximation. Within the framework of this approximation electronic energy levels are found for fixed nuclei configuration. The electronic energy obtained as a function of nuclei distance serves later as a potential energy surface for vibrational motion of nuclei.

The BO approximation is applicable whenever the energy distance between the electronic states is larger then the coupling term between them. In such a case nucleus move on a single electronic potential surface and the coupling to the others can be neglected. However for fixed internuclear distances $R < 3.2a.u.$ the H_2^- intermediate formed in the e/H_2 collision process has no bound states. Due to the autoionization process it supports only continuum states. The distance between the electronic states of continuum is zero, hence the usual BO approximation would require dealing with an immense number of electronic potential surfaces strongly coupled with each other.

For a fixed $H - H$ distance the H_2^- molecule decays exponentially with a rate depending on that distance. This exponential decay can be described

by a single resonance state possessing a *complex* electronic "energy". The real part of the complex eigenvalue is the energy position of the resonance state and the imaginary part is proportional to its decay rate (inverse lifetime). *From here follows that instead of using many real coupled electronic potential surfaces within the BO approximation we can solve the nuclear Schrödinger equation with a single complex potential energy surface.*

We will derive here the expression for the vibrational excitation cross section of electron/molecule collision using the complex adiabatic approximation. Let us consider a scattering event where the electron represented by $\sqrt{\frac{1}{k_i}}e^{ik_i r}$, collides with a molecule which has N internal electrons. We assume that the electronic state of the molecule is varied adiabatically during the collision. The molecular degrees of freedom are represented by coordinate R. Prior to collision the molecule is in its ν vibrational state, $\chi_\nu(R)$, and in its n_0-th electronic state, $\phi_{n_0}(\{r\}_N; R)$. Assuming adiabaticity, the initial state, $\chi_\nu(R)\Phi_i(\{r\}_{N+1}; R)$, properly antisymmetrized in the electronic coordinates such that

$$\Phi_i(\{r\}_{N+1}; R) = \mathcal{A}(\phi_i(\{r\}_N; R)\sqrt{\frac{1}{k_i}}e^{ik_i r_{N+1}}) \tag{1}$$

is an eigenfunction of the interaction free Hamiltonian

$$H_0 = T(R) + T(\{r\}_{N+1}) + V_{mol}(\{r\}_N, R) \tag{2}$$

where $T(\{r\}_{N+1})$ and $T(R)$ are respectively electronic and nuclear kinetic energy operators and $V_{mol}(\{r\}_N, R)$ is the potential energy of the N electrons and nucleus of the molecule. After the inelastic collision the molecule is found in its vibrationally excited state $\chi_{\nu'}(R)$ and the scattered electron is in a state defined by $\sqrt{\frac{1}{k_f}}e^{ik_f r_{N+1}}$. The final state of the non interacting electron-molecule system is $\chi_{\nu'}(R)\Phi_f(\{r\}_{N+1}; R)$ where

$$\Phi_f(\{r\}_{N+1}; R) = \mathcal{A}(\phi_f(\{r\}_N; R)\sqrt{\frac{1}{k_f}}e^{ik_f r_{N+1}}). \tag{3}$$

The energy of the scattered electron is given by the energy conservation law:

$$\frac{|\hbar k_i|^2}{2m_e} + E_\nu = \frac{|\hbar k_f|^2}{2m_e} + E'_\nu \equiv E \tag{4}$$

where m_e is the mass of an electron, E_ν and E'_ν are the energies of the initial and the final states of the molecule. The Hamiltonian during the collision process is given by,

$$H = T(R) + T(\{r\}_{N+1}) + V_{int}(\{r\}_{N+1}, R) \tag{5}$$

where V_{int} is the $N+1$ electron and nucleus interaction potential. V_{int} includes the coordinates of both the colliding electron and the electrons of the molecule. Since the electronic coordinate is much faster than the molecular one the Born-Oppenheimer (BO) approximation is applicable here. The adiabatic BO Hamiltonian is defined by

$$H_{ad}(\{r\}_{N+1};R) = T(\{r\}_{N+1}) + V_{int}(\{r\}_{N+1};R) \tag{6}$$

where the nuclear coordinate R is a parameter. The adiabatic Hamiltonian H_{ad} possesses R-dependent eigenenergies $E_n^{ad}(R)$ and eigenfunctions $\phi_n^{ad}(\{r\}_{N+1};R)$ such that

$$H_{ad}(\{r\}_{N+1};R)\phi_n^{ad}(\{r\}_{N+1};R) = E_n^{ad}(R)\phi_n^{ad}(\{r\}_{N+1};R). \tag{7}$$

The adiabatic energy $E_n^{ad}(R)$ serves as a potential for the motion of the heavy nuclei:

$$(T(R) + E_n^{ad}(R))\chi_{n,\alpha}^{ad}(R) = \epsilon_{n,\alpha}^{ad}\chi_{n,\alpha}^{ad}(R) \tag{8}$$

where $\chi_{n,\alpha}^{ad}(R)$ and $\epsilon_{n,\alpha}^{ad}$ are the nuclear vibrational wave function and energy. Within the Born-Oppenheimer approximation the total wave function is a product of the nuclear wave function and the electronic wave function which depends parametrically on the nuclear coordinate:

$$\Psi_{n,\alpha}^{ad} = \phi_n^{ad}(\{r\}_{N+1};R)\chi_{n,\alpha}^{ad}(R) \tag{9}$$

According to the Lippman-Schwinger equation the probability to change the vibrational state of the molecule from $\chi_\nu(R)$ to $\chi_{\nu'}(R)$ due to the collision process is given by,

$$\sigma = |\langle\Psi_f|V + VGV|\Psi_i\rangle|^2 \tag{10}$$

where respectively the initial and the final states are given by:

$$\Psi_i = \chi_\nu(R)\Phi_i(\{r\}_{N+1};R) \quad \Psi_f = \chi_{\nu'}(R)\Phi_f(\{r\}_{N+1};R). \tag{11}$$

V is defined as $V = V_{int} - V_{mol}$. The resonant part of the excitation probability is

$$\sigma_{res} = \left|\lim_{\epsilon\to 0^+}\left\langle \chi_{\nu'}(R)\Phi_i(\{r\}_{N+1};R)\left|V\frac{1}{E-H+i\epsilon}V\right|\right.\right. \\ \left.\left.\chi_\nu(R)\Phi_f(\{r\}_{N+1};R)\right\rangle_{r,R}\right|^2. \tag{12}$$

Using the spectral representation of the Green operator $(E - \hat{H})^{-1}$ in Eq. (12) within the Born-Oppenheimer approximation framework one gets:

$$\sigma_{res} = \left| \sum_{n,\alpha} \frac{\left\langle \chi_{\nu'} \left| \left\langle \Phi_i | V | \Psi^{ad}_{n,\alpha} \right\rangle_r \left\langle \Psi^{ad}_{n,\alpha} | V | \Phi_f \right\rangle_r \right| \chi_\nu \right\rangle_R}{E - E^{ad}_{n,\alpha}} \right|^2 \tag{13}$$

The molecular anion, which is formed when an electron collides with a neutral molecule, supports no bound states. However, the electron can be trapped for a finite period of time in the quasibound resonance state. As was mentioned above, there are several methods, such as complex scaling (CS), which allow us to "concentrate" the information about the resonance phenomena into a *single square integrable state* which is associated with a complex energy eigenvalue, $E^{res}_n = \epsilon_n - \frac{i}{2}\Gamma_n$. That is, $\hat{H}_{CS}|n\rangle = E^{res}_n|n\rangle$ where $\hat{H}_{CS}$ is the complex scaled Hamiltonian. The solution space of the complex scaled molecular anion Hamiltonian can be divided into subspace of resonance states and into the subspace of continuum scattering states. Whenever the resonance is isolated (the distance between two consecutive resonances is larger then the width, Γ of each resonance) and has a large lifetime ($\Gamma/\hbar$ is larger than any characteristic frequency of the system) we can make an assumption that a scattering event involves a single resonance state.

A common situation is that, $\Delta E_{vib} \leq \Gamma < \Delta E_{elec}$ where ΔE_{elec} and ΔE_{vib} are respectively the energy spacing between electronic levels and vibrational levels. In such a case scattering event proceeds via a single *electronic* resonance state, n_0. However it involves a number of vibrational states $\{\chi^{ad}_\nu\}$ belonging to the same electronic resonance state, n_0. Consequently the sum over electronic energy levels, n, can be omitted from the sum in the expression for the resonant part of the excitation probability in Eq. (13):

$$\sigma_{res} = \left| \sum_{\alpha}^{res} \frac{\left\langle \chi_{\nu'} \left\langle \Phi_i | V | \phi^{ad}_{n_0} \right\rangle_r \chi^{ad}_{n_0,\alpha} \right\rangle_R \left\langle \chi^{ad}_{n_0,\alpha} \left\langle \phi^{ad}_{n_0} | V | \Phi_f \right\rangle_r \chi_\nu \right\rangle_R}{E - E^{ad}_{n_0,\alpha}} \right|^2 \tag{14}$$

Moiseyev and Peskin [11] have shown that the integrals over the electronic coordinates in the Eq. (14) are related to the partial widths. That is,

$$\begin{aligned} \left| \left\langle \Phi_i | V | \phi^{ad}_{n_0}(\{r\}_{N+1}; R) \right\rangle_r \right|^2 &= \Gamma^{(i)}_{n_0}(R) \\ \left| \left\langle \Phi_f | V | \phi^{ad}_{n_0}(\{r\}_{N+1}; R) \right\rangle_r \right|^2 &= \Gamma^{(f)}_{n_0}(R) \end{aligned} \tag{15}$$

where $\Gamma^{(i)}_{n_0}(R)$ is the partial width of the electronic resonance state n_0 as function of the nuclear coordinate R. The products of this decay channel

are neutral molecule and a free electron associated with a wave number k_i. $\Gamma_{n_0}^{(f)}(R)$ is the partial width for the decay channel that results in a neutral molecule and a scattered electron associated with k_f wave number.

Within the local approximation the energy dependence of the partial widths (via the scattered electron wave number k) is neglected and $\Gamma_{n_0}^{(i)} = \Gamma_{n_0}^{(f)}$. Using this approximation and Eqs. (14, **??**) one gets that:

$$\sigma_{res} = \left| \sum_{\alpha}^{res} \frac{\left\langle \chi_{\nu'} | \Gamma_{n_0}^{\frac{1}{2}}(R) | \chi_{n_0,\alpha}^{ad} \right\rangle_R \left\langle \chi_{n_0,\alpha}^{ad} | \Gamma_{n_0}^{\frac{1}{2}}(R) | \chi_{\nu} \right\rangle_R}{E - E_{n_0,\alpha}^{ad}} \right|^2 \tag{16}$$

Since Γ_{n_0} is the width of the electronic resonance state n_0 it is related to the imaginary part of the adiabatic electronic energy $E_{n_0}^{ad}$:

$$\Gamma_{n_0}(R) = -2Im\ E_{n_0}^{ad}(R) \tag{17}$$

Equation (16) given above not only simplifies the calculation of σ but also provides a simple physical insight to the problem of electron scattering from a neutral molecule. Since the final expression for the vibrational excitation cross section does not depend on the electron coordinates we can say that the electron-neutral molecule collision prepares a nuclear wave packet on the potential energy surface of the molecular anion intermediate. The prepared wave packet is propagated via the nuclear Born-Oppenheimer molecular anion Hamiltonian with the complex potential $E_{n_0}^{ad}(R)$. Finally, the anion undergoes autionization process resulting in the molecule in a vibrationally excited state. The probability amplitude to obtain a specific vibrational state ν of the molecule is given in Eq. (16). This expression is in a complete agreement with the results obtained by Domcke and Cederbaum [12] by applying the local approximation to the exact expression for σ.

(ii) *interatomic Coulombic decay of* $\left[Ne_2^+\right]^*$

We will demonstrate here an application of the complex analogue of the Born-Oppenheimer approximation to a half collision process, namely, to the reaction

$$Ne_2 + \hbar\omega \rightarrow \left[Ne_2^+\right]^* + e^- \rightarrow \left[Ne_2^{2+} + e^-(\text{ICD})\right] + e^- \rightarrow 2Ne^+ + 2e^-,$$

where the electronically excited cationic dimer, $\left[Ne_2^+\right]^*$, has a hole in its inner-valence 2s-type molecular orbital $2^2\Sigma_u^+$. We will present the derivation of the expressions for the kinetic energy distributions of the emitted interatomic Coulombic decay electron and of the Ne^+ fragments.

Within the framework of the Born-Oppenheimer approximation the initial state, that is, the ground state of neutral neon dimer, is given by

$$\Psi_0[\mathrm{Ne_2}](\{\vec{\mathrm{r}}\}_\mathrm{N},\mathrm{R}) = \psi^{\mathrm{elec}}[\mathrm{Ne_2}](\{\vec{\mathrm{r}}\}_\mathrm{N};\mathrm{R})\chi_0[\mathrm{Ne_2}](\mathrm{R}). \tag{18}$$

$N = 20$ is the number of electrons, $\{\vec{r}\}_N$ is the notation for the coordinates of the N electrons, $\psi^{\mathrm{elec}}[\mathrm{Ne_2}]$ is the adiabatic electronic wave function in the electronic ground state of $\mathrm{Ne_2}$, and $\chi_0[\mathrm{Ne_2}]$ is the vibrational eigenfunction of the nuclear Hamiltonian with the electronic ground state potential energy surface.

Utilizing electromagnetic radiation from a synchrotron source, for instance, an inner-valence electron can be ejected and a superposition of autoionizing states of $\mathrm{Ne_2^+}$ in the $2^2\Sigma_u^+$ electronic state is generated. We can approximate these resonance states by the BO solutions only when the non Hermitian approach is taken and the potential energy surface obtained from the electronic structure calculations is complex, $E[2^2\Sigma_u^+\mathrm{Ne_2^+}](R) = \mathrm{Re}E[2^2\Sigma_u^+\mathrm{Ne_2^+}](R) - \frac{i}{2}\Gamma[2^2\Sigma_u^+\mathrm{Ne_2^+}](R)$. Under these circumstances the autoionizing states of $\left[\mathrm{Ne_2^+}\right]^*$ can be factorized into an electronic and a nuclear part,

$$\begin{aligned}\Psi_\nu[2^2\Sigma_u^+\mathrm{Ne_2^+}](\{\vec{r}\}_{N-1},R) = \\ \psi^{\mathrm{elec}}[2^2\Sigma_u^+\mathrm{Ne_2^+}](\{\vec{r}\}_{N-1},R)\chi_\nu[2^2\Sigma_u^+\mathrm{Ne_2^+}](R).\end{aligned} \tag{19}$$

Exposing $\mathrm{Ne_2}$ to radiation with photon energy $\hbar\omega$ significantly above the inner-valence ionization threshold can lead to formation of a wave packet of the $(N-1)$-electron system $\left[\mathrm{Ne_2^+}\right]^*$,

$$\begin{aligned}\Phi^{\mathrm{WP}}[2^2\Sigma_u^+\mathrm{Ne_2^+}](\{\vec{r}\}_{N-1},R) = \\ \sum_\nu \left(\chi_\nu[2^2\Sigma_u^+\mathrm{Ne_2^+}]|\mu(R)|\chi_0[\mathrm{Ne_2}]\right)_R \Psi_\nu[2^2\Sigma_u^+\mathrm{Ne_2^+}](\{\vec{r}\}_{N-1},R),\end{aligned} \tag{20}$$

and a photoelectron in state ϕ_{PE}, which in the sudden approximation does not interact with the $\mathrm{Ne_2^+}$ cation. Thus the dipole transition moment $\mu(R)$ is given by

$$\mu(R) = \left(\mathcal{A}\{\psi^{\mathrm{elec}}[2^2\Sigma_u^+\mathrm{Ne_2^+}]\phi_{\mathrm{PE}}\}|e\sum_{i=1}^{N}\vec{r}_i\cdot\vec{e}_z|\psi^{\mathrm{elec}}[\mathrm{Ne_2}]\right)_{\vec{r}}, \tag{21}$$

where $(\cdot|\cdot)_{\vec{r}}$ indicates integration over the electronic coordinates, e denotes the charge of an electron, and $\vec{e}_z$ is a unit vector along the polarization axis of linearly polarized light. The symbol $\mathcal{A}$ is used to emphasize that the product state of cation and photoelectron must be properly antisymmetrized.

The wave packet $\Phi^{\mathrm{WP}}[2^2\Sigma_u^+\mathrm{Ne}_2^+]$ undergoes electronic decay according to the ICD mechanism. The products of this relaxation process are dissociative Ne_2^{2+} in its electronic ground state and a free ICD electron in state ϕ_{ICD} with kinetic energy E_{kin}. Within the framework of the BO approximation the final states can be written as

$$\Psi_f[\mathrm{Ne}_2^{2+} + e^-(\mathrm{ICD})](\{\vec{r}\}_{N-1}, R) = \mathcal{A}\{\phi_{\mathrm{ICD}}\psi^{\mathrm{elec}}[\mathrm{Ne}_2^{2+}]\}(\{\vec{r}\}_{N-1}; R)\chi_{E_f}[\mathrm{Ne}_2^{2+}](R). \tag{22}$$

The dissociative nuclear wave functions $\chi_{E_f}[\mathrm{Ne}_2^{2+}]$ are associated with continuous energies $E_f[\mathrm{Ne}_2^{2+}]$. Then the energy of the state $\Psi_f[\mathrm{Ne}_2^{2+} + e^-(\mathrm{ICD})]$ is $E_{kin} + E_f[\mathrm{Ne}_2^{2+}]$.

We treat the coupling between the ICD electron and the dication by means of the Lippmann-Schwinger equation extended to non Hermitian Hamiltonians:

$$\Phi_f[\mathrm{Ne}_2^+] = (1 + \hat{G}(E_{kin} + E_f[\mathrm{Ne}_2^{2+}])\hat{V})\Psi_f[\mathrm{Ne}_2^{2+} + e^-(\mathrm{ICD})]. \tag{23}$$

$\left(\Phi^{\mathrm{WP}}[2^2\Sigma_u^+\mathrm{Ne}_2^+]|\Phi_f[\mathrm{Ne}_2^+]\right)$ is the probability amplitude that the wave packet $\Phi^{\mathrm{WP}}[2^2\Sigma_u^+\mathrm{Ne}_2^+]$ decays into Ne_2^{2+} with energy $E_f[\mathrm{Ne}_2^{2+}]$ and an ICD electron with energy E_{kin}. The expression explicitly reads

$$\left(\Phi^{\mathrm{WP}}[2^2\Sigma_u^+\mathrm{Ne}_2^+]|\Phi_f[\mathrm{Ne}_2^+]\right) = \sum_\nu \left(\chi_0[\mathrm{Ne}_2]|\mu(R)|\chi_\nu[2^2\Sigma_u^+\mathrm{Ne}_2^+]\right)_R \cdot \frac{\left(\Psi_\nu[2^2\Sigma_u^+\mathrm{Ne}_2^+]|\hat{V}|\Psi_f[\mathrm{Ne}_2^{2+} + e^-(\mathrm{ICD})]\right)_{\vec{r},R}}{E_{kin} + E_f[\mathrm{Ne}_2^{2+}] - E_\nu[2^2\Sigma_u^+\mathrm{Ne}_2^+]} \tag{24}$$

What remains to be discussed is the determination of the interaction matrix elements $\left(\Psi_\nu[2^2\Sigma_u^+\mathrm{Ne}_2^+]|\hat{V}|\Psi_f[\mathrm{Ne}_2^{2+} + e^-(\mathrm{ICD})]\right)_{\vec{r},R}$. $\hat{V}$ is defined as

$$\hat{V} = \hat{H}[2^2\Sigma_u^+\mathrm{Ne}_2^+] - \hat{H}[\mathrm{Ne}_2^{2+} + e^-(\mathrm{ICD})]. \tag{25}$$

where $\hat{H}[2^2\Sigma_u^+\mathrm{Ne}_2^+]$ is a complex, non Hermitian Hamiltonian whereas $\hat{H}[\mathrm{Ne}_2^{2+} + e^-(\mathrm{ICD})]$ is Hermitian. By using the BO expressions for $\Psi_\nu[2^2\Sigma_u^+\mathrm{Ne}_2^+]$ (Eq. (19)) and $\Psi_f[\mathrm{Ne}_2^{2+} + e^-(\mathrm{ICD})]$ (Eq. (22)) it is straightforward to derive that

$$\left(\Psi_\nu[2^2\Sigma_u^+\mathrm{Ne}_2^+]|\hat{V}|\Psi_f[\mathrm{Ne}_2^{2+} + e^-(\mathrm{ICD})]\right)_{\vec{r},R} = \left(\chi_\nu[2^2\Sigma_u^+\mathrm{Ne}_2^+]|d(R)|\chi_{E_f}[\mathrm{Ne}_2^{2+}]\right)_R, \tag{26}$$

where

$$d(R) = \left(\psi^{\mathrm{elec}}[2^2\Sigma_u^+\mathrm{Ne}_2^+]|\hat{V}|\mathcal{A}\{\phi_{\mathrm{ICD}}\psi^{\mathrm{elec}}[\mathrm{Ne}_2^{2+}]\}\right)_{\vec{r}}. \tag{27}$$

Moiseyev and co-workers have shown [8, 11] that, apart from a multiplicative constant, in the local approximation

$$d(R) = e^{i\varphi(R)}\sqrt{\Gamma(R)}. \tag{28}$$

Here $\Gamma(R) = \Gamma[2^2\Sigma_u^+ \mathrm{Ne}_2^+](R)$ is the local electronic decay width of inner-valence ionized neon dimer and $\varphi(R)$ is the phase of the resonance width amplitude.

The kinetic energy distribution of the ICD electrons, $\sigma(E_{kin})$, is obtained by adding up all decay probabilities $\left|\left(\Phi^{\mathrm{WP}}[2^2\Sigma_u^+\mathrm{Ne}_2^+]|\Phi_f[\mathrm{Ne}_2^+]\right)\right|^2$ that are associated with an ICD electron of energy E_{kin} in the final state,

$$\sigma(E_{kin}) = \int dE_f[\mathrm{Ne}_2^{2+}] \left|\left(\Phi^{\mathrm{WP}}[2^2\Sigma_u^+\mathrm{Ne}_2^+]|\Phi_f[\mathrm{Ne}_2^+]\right)\right|^2. \tag{29}$$

Assuming $\mu(R) = 1$ and $\varphi(R) = 1$, Eq. (16) follows immediately by inserting Eqs. (24), (26), and (28) into Eq. (29). In a similar fashion the kinetic energy distribution of the Ne^+ fragments, $\tilde{\sigma}(E_f)$, is given by

$$\tilde{\sigma}(E_f) = \int dE_{kin} \left|\left(\Phi^{\mathrm{WP}}[2^2\Sigma_u^+\mathrm{Ne}_2^+]|\Phi_f[\mathrm{Ne}_2^+]\right)\right|^2. \tag{30}$$

3. Physical phenomena explained by non Hermitian quantum mechanics

3.1. FINGERPRINTS OF OVERLAPPING RESONANCES IN ELECTRON-HYDROGEN SCATTERING CROSS-SECTION MEASUREMENTS

In this section we will propose a mechanism that leads to the structure in the cross section even when the resonances are overlapping i.e. $\Gamma_n > |\epsilon_n - \epsilon_{n\pm1}|$ where ϵ_n is the energy position of the resonance state and Γ_n is the corresponding width. We will describe a case where the *interference* among resonance states results in sharp structure in the scattering cross section σ. This is very different from the known Fano interferences [13] which take place between a given resonance state and a weakly energy dependent background. Fano interferences lead to the distortion of the shape of the resonance peak in the cross section but not to a substantial increase of the lifetime of the trapped particle in the scattering process. In our case the structure is the result of the interference among resonances and consists of peaks where each one of them is much narrower than the width of a single resonance state Γ_n. Since the lifetime of the trapped particle is proportional to the inverse of the width of the peak in the cross section, it implies that the narrowing of the peak in the cross section increases the lifetime of the

trapped particle. Moreover, the interference takes place between many resonances which are separated by a large energy interval as compared to the corresponding resonance widths i.e., $|\epsilon_n - \epsilon_m| \gg Max(\Gamma_n, \Gamma_m)$. *Therefore we may consider the new mechanism presented here as a collective coherent resonance phenomenon.* As it will be discussed below, this phenomenon was first observed, without realizing it, in the experiments of inelastic electron scattering from an H_2 molecule [14]. The sharp structure in the experimental electron/hydrogen-molecule scattering cross section is associated with the short-lived vibrational states of the autoionizing H_2^- intermediate. We have calculated the positions and the widths of these H_2^- states within the local approximation and to our surprise we obtained that the width of the resonance states were 2-3 times larger than the widths of the peaks in the vibrational excitation cross sections [1]. Yet, the mechanism that leads to this phenomenon remained unclear.

We will show here that the nuclear motion of H_2^- induces interference between resonances such that the structures appearing in the scattering cross section are narrower than the width of a single resonance state, Γ_n. First, however, we would like to stress that the interference phenomenon between the resonance states itself is associated with the generalization of the inner product in quantum mechanics. This generalization is required when resonances, metastable states, are associated with complex, rather than real eigenvalues of the Hamiltonian.

The transition probability amplitude, $t(E)$, for a scattering experiment where the initial and the final states are identical, i.e. $|\phi_i\rangle = |\phi_f\rangle = |0\rangle$, is given by the Lippmann-Schwinger equation,

$$t(E) = \langle 0|V + VGV|0\rangle = t_{direct}(E) + t_{res}(E) \tag{31}$$

The resonant term, $t_{res}(E)$, is given by

$$t_{res}(E) = \int d\epsilon\, \rho(\epsilon) a(\epsilon)/(E - \epsilon), \tag{32}$$

where $\hat{H}|\epsilon\rangle = \epsilon|\epsilon\rangle$, $a(\epsilon) = |\langle 0|V|\epsilon\rangle|^2 \geq 0$ and $\rho(\epsilon)$ stands for the density of states. However, when $\hat{H}$ is an Hermitian operator the eigenvalues, ϵ, get real values only and the information about the resonance phenomena is spread over a large number of continuum states. Using the complex scaling (CS) method allows us to "concentrate" the information about the resonance phenomena into a *single square integrable state* which is associated with a complex energy eigenvalue, $E_n^{res} = \epsilon_n - \frac{i}{2}\Gamma_n$. That is, $\hat{H}|n\rangle = E_n^{res}|n\rangle$ where $|n\rangle$ is an eigenfunction which is *not* in the Hermitian domain of the Hamiltonian H. This enables us to replace the integral in the expression

for the $t_{res}(E)$ by a sum over the discrete resonance states,

$$t_{res}(E) = \sum_n a_n/(E - \epsilon_n + \frac{i}{2}\Gamma_n). \tag{33}$$

Since the eigenfunction $|n\rangle$ is not in the Hermitian domain of the Hamiltonian the definition of the inner product that we should use should be questioned. If we will keep the usual definition of the scalar product in quantum mechanics the coefficients a_n in Eq. 33 will get real positive values only (as well as $a(\epsilon)$ in Eq. 32) and the possibility of interference among different resonance states which leads to the trapping of an electron due to the molecular vibrations will be eliminated. As was mentioned before the generalized definition of the inner product (...|...) rather than the usual scalar product $\langle ...|... \rangle$ has to be used since the Hamiltonian is not Hermitian [5, 6]. Only the application of the generalized inner product can give rise to the complex coefficients, $a_n = (0|V|n)(n|V|0)$, in Eq. 33. The fact that $\{a_n\}$ can get complex and real negative values is essential to obtain the interference phenomenon which increases the lifetime of H_2^- intermediate in the e^-/H_2 scattering experiments.

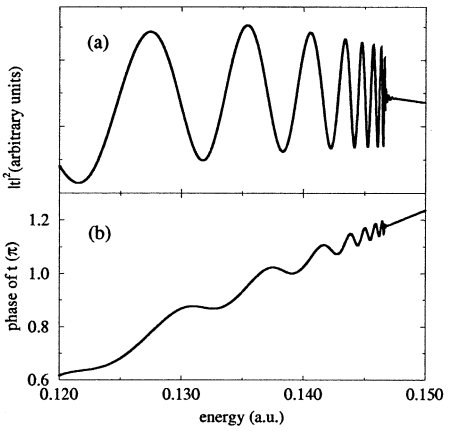

Figure 1. (a) The behavior of the probability to excite H_2 molecule from the ground vibrational $\nu = 0$ to the $\nu = 4$ excited state in e/H_2 collision. (b) The phase of the corresponding probability amplitude.

In Figs 1 a,b we represent the electron-H_2 scattering cross section and the phase of the corresponding excitation probability amplitude. The widths of the peaks in Fig. 1a are $2 - 3$ times narrower than the width of the H_2^- resonance states. The phase shows an oscillatory behavior similar to the behavior of the transition probability amplitude phase as measured in the experiments of an electron passing through a quantum dot [15].

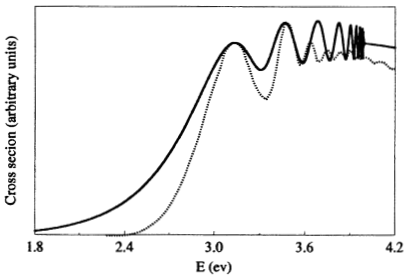

Figure 2. Solid line shows the calculated probability to excite H_2 molecule from the ground vibrational $\nu = 0$ to the $\nu = 4$ excited state in e/H_2 collision. Dotted line represents the shifted experimental results.

Note that our numerical results presented in Fig. 2 are in a remarkable semiquantative agreement with the experimental cross section [14]. The experimental cross section was shifted up in energy by 0.45 *ev* to emphasize the agreement between the vibrational structures seen in the spectrum. Similar agreement was obtained earlier by Mündel et. al. [16] using a different approach.

We will now give a more detailed description of the electron trapping phenomena and show that it is associated with the self-orthogonality phenomenon. It is known that the ${}^2\Sigma_u^+$ resonance of H_2^- which is responsible for the vibrational excitation in the low energy region, is an extremely short-lived resonance with a lifetime comparable with the duration of the non resonant scattering [17].

For a fixed $H - H$ distance the H_2^- molecule autoionizes with a rate depending on the $H - H$ bond length, $\Gamma(R)$. This exponential decay can be described by a single resonance state possessing a *complex* electronic "energy" $V(R) - \frac{i}{2}\Gamma(R)$ (see Fig. 3) [18].

Therefore instead of using many real coupled electronic potential surfaces within the Born-Oppenheimer approximation we can solve the nuclear Schrödinger equation with a single complex potential energy surface [1], $\widehat{H} = \widehat{T}_{nuclear} + V(R) - \frac{i}{2}\Gamma(R)$.

By solving the nuclear H_2^- Schrödinger equation with the complex potential surface we obtained two distinctive types of resonance states which are presented in Fig. 3. The first one is associated with vibrationally bound motion of autoionizing H_2^- molecule, i.e. $H_2^- \rightarrow H_2 + e^-$. We will refer to these states as vibrationally-discrete autoionization-resonance states. The

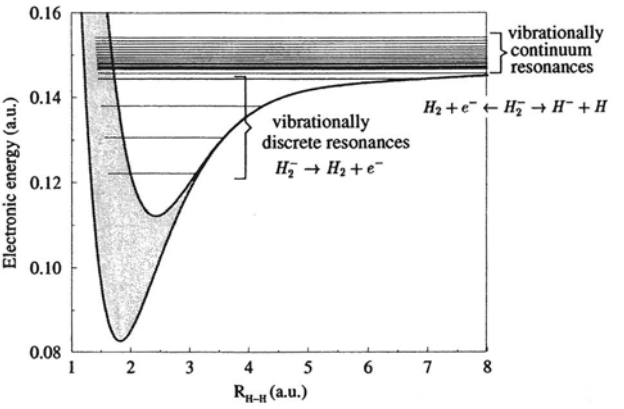

Figure 3. The shaded area describes the electronic "energy" $\epsilon(R) \pm \Gamma(R)/2$ of autoionizing H_2^- as a function of the internuclear distance R. The horizontal parallel lines stand for the autionization resonance energy levels (the resonance widths are not shown here). The continuum part of the spec trum is quantized due to the finite box approximation.

second type of states is associated with the free motion of the nuclei and is referred to here as vibrationally-continuum autoionization-resonances where $H_2(bound) + e^- \overset{A}{\leftarrow} H_2^-(continuum) \overset{B}{\rightarrow} H^- + H$ (i.e. a branch cut of autoionizing states). Note that the autoionization (A) takes place at the inner classical turning point where the width of the complex potential surface is the largest. The dissociation (B) occurs at the outer region where the width of the complex potential is zero. As we will show below the formation of branch cut of resonances due to the nuclear motion plays the key role in the mechanism which is responsible for the enhancement of the electron trapping by the hydrogen molecule.

The initial state populates both types of resonance states of H_2^-. Interference between the vibrational discrete and the vibrational continuum autoionization resonances takes place although the resonance positions of the vibrationally-discrete autoionization-resonance (disc-res) states and the vibrationally-continuum autoionization-resonance states (cont-res) are very "far" from one another (as compared to their width). One may think that when $E \sim \epsilon_n(disc-res)$ there is only one dominant term in the series resonance expansion of $t_{res}(E)$ (see Eq. 33). This is however not the case. The numerators associated with the branch-cut resonances, $a_n(cont-res)$, get complex values where both the real and the imaginary parts are larger than the corresponding ones of $a_n(disc-res)$ by *several orders of magnitude.* In the numerical calculations the amplitudes of the continuum type resonances

were found to be larger by 8-10 orders of magnitude than the discrete type resonance amplitudes. Consequently, $|a_n(cont-res)| >> |a_{n'}(disc-res)|$ but, however, at $E = E_n(disc-res)$,

$$\left|\frac{a_n(disc-res)}{\frac{i}{2}\Gamma_n(disc-res)}\right| \approx \left|\frac{a_{n'}(cont-res)}{\Delta E + \frac{i}{2}\Gamma_{n'}(cont-res)}\right| \tag{34}$$

where

$$\Delta E = E_n(disc-res) - E_{n'}(cont-res) \tag{35}$$

even when the difference between the $H_2^-(disc-res) \rightarrow H_2 + e^-$ resonances and $H_2 + e^- \leftarrow H_2^-(cont-res) \rightarrow H^- + H$ resonances is much larger then the corresponding resonance widths,

$$\Delta E \gg Max(\Gamma_n, \Gamma_{n'}).$$

The number of dominant terms in the expression for $t_{res}(E)$ (Eq. 33) determines the number of effective indirect scattering events in the scattering experiment. In our case due to the large amplitudes of the branch-cut (continuum) resonances this number is large and therefore we deal with a multiple scattering process and a collective resonance phenomenon. By collectiveness we mean that even at the resonance energy, $E = \epsilon_n$, a large number of resonances have dominant contributions to the expansion of t_{res} given in Eq. 33.

The large amplitude of the continuum resonance states is a direct result of the non Hermitian properties of H_2^- Hamiltonian (i.e. the resonance eigenfunctions which are associated with complex eigenvalues are not in the Hermitian domain of the molecular Hamiltonian). Let us explain this point in some more detail. As was mentioned above Moiseyev and Friedland [7] have proved that if two $N \times N$ real symmetric matrices H_1 and H_2 do not commute, there exists at least one value of parameter $\lambda = \lambda_b$ such that matrix $H_1 + \lambda H_2$ possesses incomplete spectrum. That is at $\lambda \rightarrow \lambda_b$ there are at least two specific eigenstates i and j for which $\lim_{\lambda\rightarrow\lambda_b}(\epsilon_i - \epsilon_j) = 0$ and also $\lim_{\lambda\rightarrow\lambda_b}(\psi_i - \psi_j) = 0$. Since ψ_i and ψ_j are orthogonal (within the general inner product definition i.e., $(\psi_i|\psi_j) \equiv \langle\psi_i^*|\psi_j\rangle = 0$ and not in the usual scalar product definition) upon coalescence their length is reduced to zero $\langle\psi_i^*|\psi_i\rangle = \varepsilon$, $\varepsilon \rightarrow 0$. When $\lambda \neq \lambda_b$ but is very close to it we still require normalization of ψ_i, $\langle\psi_i^*|\psi_i\rangle = 1$. Therefore the components of the corresponding eigenvectors are divided by a small number $\epsilon^{1/2}$ and the amplitude of ψ_i becomes enormously large.

We will show here that the phenomenon of spectrum incompleteness is inherent in the case of H_2^-. The Hamiltonian of the intermediate H_2^- within the BO approximation is given by, $H(R) = T(R) + V(R) - \frac{i}{2}\Gamma(R)$ We can rewrite this Hamiltonian introducing an autoionization strength parameter

λ in a following way: $H(R) = T(R) + V(R) - \lambda\frac{i}{2}\Gamma(R)$. For $\lambda = 1$ we obtain the original physical Hamiltonian of H_2^-. Using real basis functions or finite grid methods the matrices representing the operators $T(R), V(R)$ and $\Gamma(R)$ are real symmetric ones. The H_2^- Hamiltonian in the matrix form is $\mathbf{H} = \mathbf{T} + \mathbf{V} - \lambda\frac{i}{2}\mathbf{\Gamma} = \mathbf{H_{Re}} - \lambda\frac{i}{2}\mathbf{\Gamma}$. Since matrices $\mathbf{H_{Re}}$ and $\mathbf{\Gamma}$ do not commute it follows from the theorem proved by Moiseyev and Friedland that there exists λ, such that the spectrum of $\mathbf{H}$ is incomplete. In order to find the values of λ where the spectrum is incomplete in the case of H_2^- we have studied the λ dependence of the spectrum. In Fig. 4 we present the spectrum of H_2^- obtained while varying λ from 0 to 1 (i.e. increasing the strength of the ionization phenomenon).

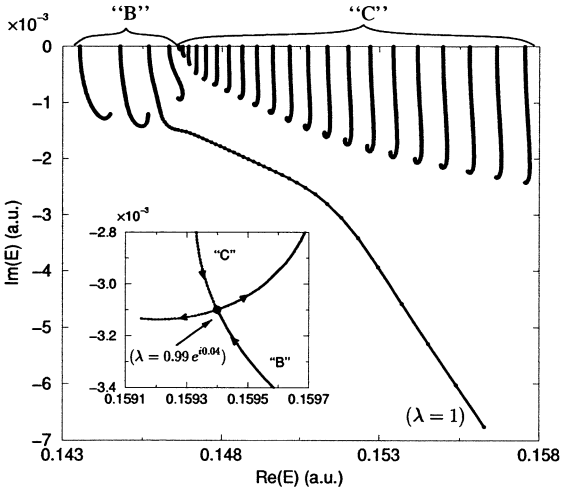

Figure 4. λ-trajectory calculations of the complex eigenvalues of $Re(\mathbf{H}) - i\lambda Im(\mathbf{H})$ where $\mathbf{H}$ is a matrix representation of the nuclear H_2^- Hamiltonian with complex electron potential surface. For $\lambda = 0$ the autoionization is artificially suppressed and the real eigenvalues obtained are divided into vibrationally bound states (denoted by "B" and into dissociative continuum solutions denoted by "C" (note that the discretization is due to the finite box approximation). The inset shows that very close to $\lambda = 1$ (the physical solution) one of the continuum solutions and the 8-th "B" solution coalesce.

There are 9 bound vibrational states of H_2^- when the autoionization process is neglected i.e. $\lambda = 0$. They all acquire finite width whenever the value of λ is increased. However the width and the position of each state changes at a very different rate. The most dramatic change occurs to the 8-th bound state ($\lambda = 0$). This state is "pushed out" above the energy threshold for the dissociation. Interestingly, whenever the position of the bound state crosses the threshold energy the behavior of the continuum

states changes as well. That is, the width of the continuum states starts to decrease with increasing λ. The reason for this behavior is that for some complex values of the parameter λ close to $\lambda = 1$ the bound state which enters the continuum part of the spectrum crosses the continuum states one by one. Since the crossing does not happen at $\lambda = 1$, the picture we see at the physical value of $\lambda = 1$ is that of avoided crossing. It should be stressed that the crossing here implies coalescence of two eigenstates, one eigenstate originating from the bound state at $\lambda = 0$ and the second one from the continuum at $\lambda = 0$. *Indeed, we found several branch points associated with the coalescence of bound and continuum states which are in the vicinity of* $\lambda = 1$. For example in the inset of Fig. 8 we show the branch point at $\lambda = 0.99145098 + i0.04006515$. The trajectory approaching from bellow is associated with the 8-th "bound" state and the trajectory approaching from above is associated with the "continuum" state. This branch point is the closest one to $\lambda = 1$ and the two states that cross at this point are very close to be self orthogonal for the physical value of $\lambda = 1$. Consequently, the amplitudes of these states are by several orders of magnitude larger then the amplitudes of the discrete resonance states that are not involved in the crossings with the continuum states. As we have shown above this effect plays a crucial role in the mechanism that leads to the electron trapping by the H_2 molecule.

We have shown in this section that the lifetime of the trapped electron in the electron scattering experiment can be dramatically increased due to the coupling between the nuclear and the electronic motions. It should be stressed that this coupling takes place between molecular autoionizing states over a very large energy range. This unusually strong coupling is due to the existence of a continuum of short lifetime autoionizing resonance states of H_2^-, located at an energy above the threshold energy of dissociation. This branch-cut of resonances is generated by the nuclear motion.

3.2. RESONANT TUNNELING PROBABILITY AMPLITUDE IN A QUANTUM DOT

Quantum dots (QD) play an important role in nano-scaled electronic devices. In order to fully understand the transport properties of quantum dots, phenomena such as tunneling of electrons must be characterized.

Phase measurements of an electron traversing a quantum dot via a double-slit interference experiment were carried out by Heiblum and his co-workers [19, 15]. In their experiment, the QD has been inserted into one slit, in a manner that enabled them to control the potential of the electrons trapped in it (by varying the plunger potential, V_p). The second slit served as a reference. The measured transition probability , $|t|^2$, oscillates as a function of the plunger potential, V_p . When the scattered elec-

tron passes through a resonance state, the transition probability exhibits a Lorentzian-shaped peak, and the phase of the transition probability amplitude changes by π, as expected by the Breit-Wigner model for resonant tunneling. Surprisingly, the phase does not accumulate but oscillates : although in each resonance the phase changes by π, between resonances it drops sharply by π. In spite of intense work on this problem [21–30] to the best of our knowledge there is no satisfactory explanation of this phenomenon. Most of the calculations which have been carried out are either for particle space model Hamiltonians or for general mathematical models based on the Friedel sum rule combined with time-reversal symmetry. The conclusion from these studies is that in true 1D systems the sharp phase drops by π in the tail of the resonant peak never occurs. Such a phenomena is obtained however, for a single electron transport for quasi-1D systems. This result obtained also in simulation calculations for a real-space model Hamiltonian with a 2D box potential (single-crossbar cavity) [25]. The discontinuity in the phase evolution of electron transport in the single crossbar cavity associated with the interference between two different transmission channels belonging to a localized state in the 2D potential and a continuous state of the transmission channel. An open question we would like to address ourselves is whether the discontinuity in the phase evolution would happen also for analytical 2D potential surfaces. Another question we would like to answer is whether the discontinuity in the phase evolution can happen due to another mechanism. As we will show here for analytical 2D potentials a sharp drop (not a discontinuity) by π happens due to the interference between adjacent resonance states associated with the double barrier potential in the adiabatic 1D potential which do not exist in the 2D single-crossbar cavity QD model Hamiltonian.

The phase drops sharply by π at transmission zeros has been associated with the fact that in quasi-1D systems the even and odd resonance levels do not necessarily alternate in energy [29, 27]. It is a common believe that whenever the transmission coefficient reaches zero, the phase has a sharp drop by π. As we will show here this is indeed a necessarily condition but not a sufficient one.

In our work we study a single electron transport for a real space 2D model Hamiltonian. The potential we introduce is a 2D one-electron effective QD model Hamiltonian that simulates the QD in Heiblum's experiment. Unlike the single-crossbar cavity used before our 2D potential is an analytical function. In our model the transition of the electron from the entrance channel to the exit one through the QD is hindered by two potential barriers that do not appear in the single-crossbar cavity model.

We obtained that for the adiabatic 1D double barrier potential, the transition probability amplitude behaves in a similar way when varying

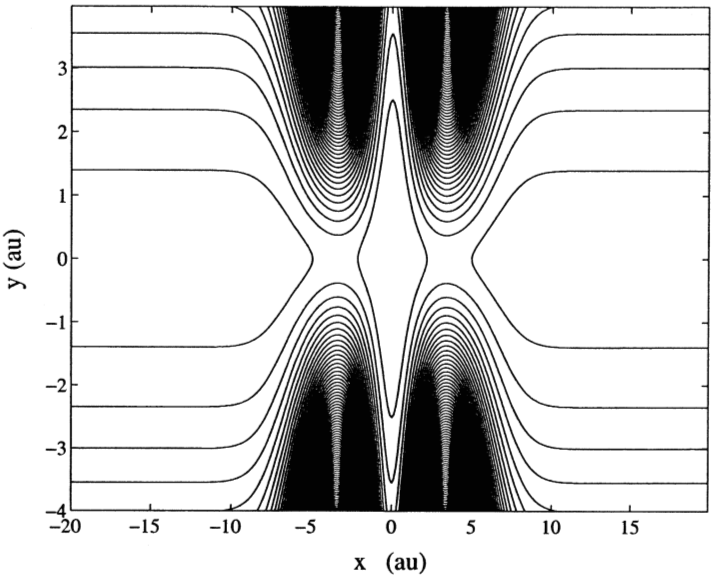

Figure 5. The two-dimensional QD potential energy surface, $V(x, y)$, defined in Eq. 37 . Note the entrance and exit channels, entrance and exit barriers and the QD embedded between the barriers. Parameters: $\mu_e = 1$;$V_0 = 0.5$; $\alpha = 1.6$; $\gamma = 0.1$; $V_p = 0$; $\lambda = 0.75$; $w_\infty = 1$; $a = 0.76215$; $b = 0.32802$; $c = 0.08871$. The parameters a, b, c were calculated according to the geometry of the QD in Heiblum's experiment. λ was chosen to allow the control on the depth of the QD well by a single parameter, V_p, without changing the height of the barriers.

the scattered electron energy, E, or the depth of the well between the two barriers (via the variation of V_p). Since the numerical calculations are simpler for the variation of the scattered electron energy rather than the variation of V_p, we address ourselves in the work presented here to the following question: how does the transition probability amplitude change as a function of the energy of the scattered electron, E, when V_p is held fixed ?

In order to answer this question we have used the complex adiabatic approach [8]. First the complex resonance potential energy surfaces (PES) were calculated as a function of the slow coordinate (which is perpendicular to the propagation coordinate). Then, assuming that the electron scattering proceeds via a single PES, the transition probability amplitude , $t(E)$, was calculated.

We propose an effective one-electron two-dimensional model potential of the QD, which preserves the main characteristics of the QD in the Heiblum experiment. That is, (a) entrance channel, entrance barrier, potential well,

exit barrier, exit channel are clearly defined (see Fig. 5); (b) similar geometrical proportions; (c) the potential surface supports at least one bound state inside the potential well, and supports isolated resonance states (i.e. $\Gamma_j < |E_j - E_{j\pm1}|$); (d) the depth of the potential well is controlled by a single parameter, the plunger potential parameter V_p, which has a minor effect on the geometry of the QD. By increasing Vp, the number of bound states in the open QD is increased.

The two-dimensional QD model Hamiltonian, where x is the propagation coordinate, is given by

$$\hat{H}(x,y) = \frac{\hat{P}_x^{\,2}}{2\mu_e} + \frac{\hat{P}_y^{\,2}}{2\mu_e} + V(x,y) \quad , \tag{36}$$

where μ_e is the effective electron mass and the potential energy surface (PES) is given by

$$V(x,y) = V(x) + \frac{\mu_e}{2} y^2 \omega^2(x) \quad , \tag{37}$$

where,

$$V(x) = V_0(x^2 - \alpha)e^{-\gamma x^2} - V_p e^{-\lambda x^2}$$

$$\omega(x) = \omega_\infty + a(x^2 - b)e^{-cx^2} \quad .$$

ω_∞ is the frequency of the harmonic motion of the free electron in the confined direction (y coordinate) in the entrance/exit channels.
The potential parameters used in our calculations are given in the caption of Fig. 5. A one dimensional cut through the PES defined above at a constant y gives a potential, $V(x;y)$, which has a well between two separated potential barriers. These 1D potentials support at least one bound state and a few isolated resonance states (see Fig. 6).

The transition probability amplitude, $t(V_p)$, in the 1D case, has been calculated using non-Hermitian scattering theory [20]. It shows a series of resonance peaks (see Fig. 6. The phase of $t(V_p)$ changes by π in resonances and accumulates between resonances (see Fig. 7. The sharp phase drop is not observed. Our calculations show that this phase drop can not be explained by 1D one-electron calculations, even when interference between different paths (different y cuts) is taken into consideration. Therefore, it is clear that two dimensions are needed to obtain the sharp phase drop phenomenon when using an effective one-electron model.

As was mentioned above, the 1D transition probability amplitude, $t(E)$, which is obtained when V_p is held fixed and the energy of the incoming electron, E, is varied, behaves similarly to the 1D transition probability amplitude $t(V_p)$. Regardless of the dimensionality of the studied problem,

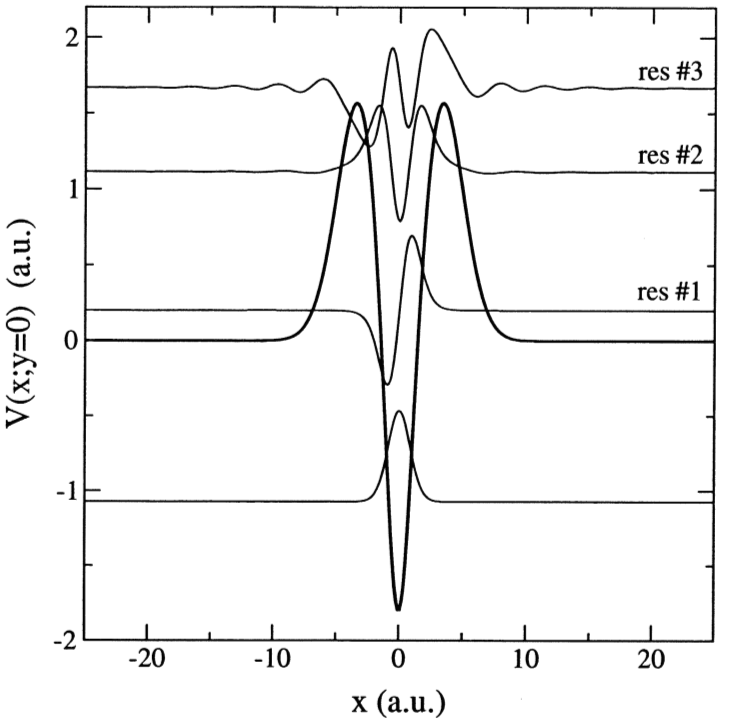

Figure 6. The 1D potential in x direction, $V(x;y=0)$, when $V_p = 1$. The Bound and isolated narrow resonance complex-scaled wavefunctions (real part) are plotted for $\theta = 0.13$.

the computational effort needed to calculate $t(V_p)$ is much larger than the one needed to calculate $t(E)$. This is because the major numerical effort lyes in the construction of the spectral representation of the Green operator, which requires the diagonalization of the Hamiltonian for every V_p. Therefore, we will concentrate on $t(E)$ in the 2D case.

We have used non-Hermitian scattering theory to calculate the transition probability amplitude, within the framework of the complex adiabatic approach. It should be stressed that non-Hermitian quantum mechanics allows us to use complex adiabatic potential energy surfaces in cases where one has to go beyond the adiabatic approximation in Hermitian quantum mechanics [1, 2]. In the adiabatic approximation, we assume that the motion in the y direction is much slower than in the x direction. This assumption is based on the geometry of the two-dimensional potential surface (see Fig. 5).

Using the adiabatic approximation, the Hamiltonian in x direction, for

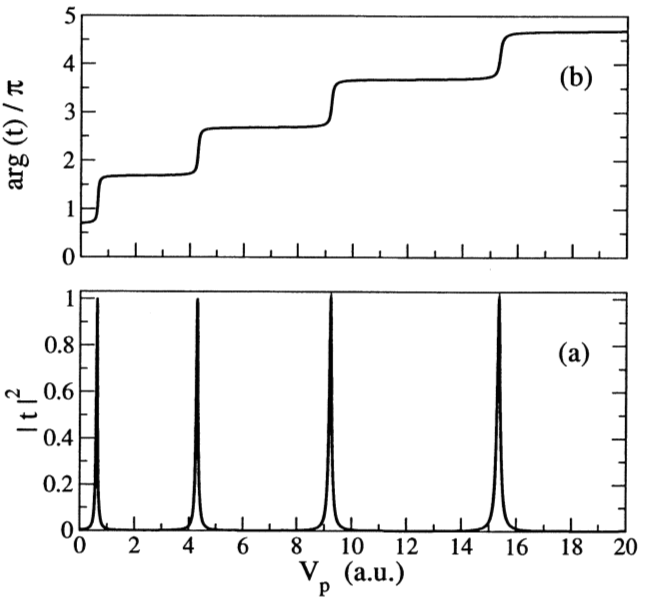

Figure 7. Transition probability for the 1D cut $V(x; y = 0)$ as a function of V_p, when the scattering energy is held fixed, $E = 1.2$ a.u. (this energy is below the barrier height for any value of V_p). (a) The transition probability, $|t|^2$, exhibits a series of peaks which correspond to the resonances. (b) The phase of the transition probability amplitude, $\arg(t)$, jumps by π in each resonance and accumulates as V_p is varied.

a given y, is given by

$$\hat{H}(x; y) = -\frac{\hbar^2}{2\mu_e}\frac{\partial^2}{\partial x^2} + V(x; y) \quad . \tag{38}$$

We use complex scaling, i.e. $x \rightarrow xe^{i\theta}$, to calculate the solutions of the complex scaled Schrödinger equation. The use of complex scaling (i.e., non-Hermitian QM) enables us to associate a resonance state with a single eigenstate of the Hamiltonian, while in Hermitian QM a resonance state is associated with a wavepacket (which is not an eigenstate of the Hermitian Hamiltonian). Therefore by complex scaling we get,

$$\hat{H}(xe^{i\theta}; y)\psi_\theta^j(x; y) = E^j(y)\psi_\theta^j(x; y) \quad . \tag{39}$$

The complex eigenenergies, $E^j(y)$, which correspond to the resonance states are θ independent, provided θ is sufficiently large. The resonance states, $\psi_\theta^j(x; y)$, are square integrable (see Fig. 6) and θ dependent.

Within the framework of the non-Hermitian adiabatic approximation separate complex resonance potential energy surfaces (PES) are defined,

$$V^j_{\text{eff}}(y) \equiv E^j(y) \equiv \varepsilon^j(y) - \frac{i}{2}\Gamma^j(y) \quad . \tag{40}$$

For the j-th resonance surface, the effective Hamiltonian in y direction is given by

$$\hat{H}_{\text{eff}}(y) = -\frac{\hbar^2}{2\mu_e}\frac{\partial^2}{\partial y^2} + V^j_{\text{eff}}(y) \quad . \tag{41}$$

By solving the eigenvalue problem,

$$\hat{H}_{\text{eff}}(y)\chi^j_n(y) = e^j_n\chi^j_n(y) \quad , \quad e^j_n \equiv \epsilon^j_n - \frac{i}{2}\gamma^j_n \tag{42}$$

the complex resonance eigenstates and eigenergies were calculated. The complex eigenergies, e^j_n, provide the energy positions, ϵ^j_n, and widths, γ^j_n (which correspond to the inverse of the lifetimes of the resonance states) of the temporarily trapped electron in the QD.

In Fig. 8 we show an effective complex resonance PES and the corresponding resonance eigenstates.

The transition probability amplitude is calculated using the Lippmann-Schwinger equation :

$$t_{i\to f}(E) = (\Psi_i|V + VGV|\Psi_f) \quad , \tag{43}$$

Where Ψ_i and Ψ_f are the initial and final wavefunctions of the scattered electron. Under the adiabatic approximation $\Psi_{i,f}$ can be presented as :

$$\Psi_{i,f}(x,y) = \Theta_{i,f}(x;y)\varphi_{i,f}(y) \quad , \tag{44}$$

where Θ is the wavefunction of the scattered electron in the x direction:

$$\Theta_{i,f}(x;y) = \sqrt{\frac{\mu_e}{\hbar^2 k_{i,f}}}e^{ik_{i,f}x} \quad , \tag{45}$$

$$k_{i,f} = \sqrt{2\mu_e(E - e^{\infty}_{i,f} - E_{th}(y))} \quad ,$$

and $\varphi_{i,f}$ are the asymptotic wavefunctions of the scattered electron in the y direction (in our case, eigenstates of a harmonic oscillator with the frequency w_∞).

Assuming tunneling is assisted by the j-th effective resonance potential surface, for the case where the quantum state of the scattered electron

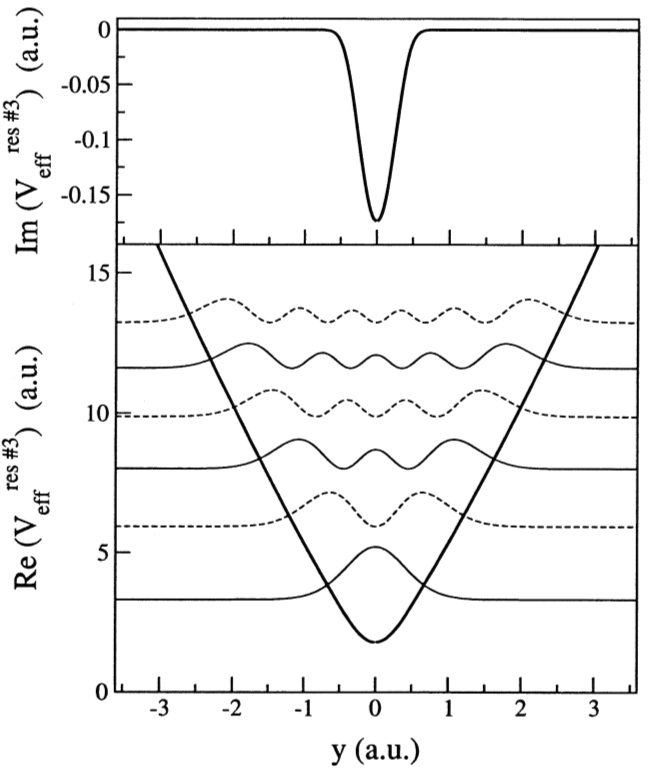

Figure 8. The 1D effective complex resonance potential energy surface (PES) in y direction, for resonance #3, when $V_p = 0$. The first 7 eigenstates, $|\chi_n^j(y)|^2$, are plotted in normal/dashed lines, according to the symmetry of the eigenstate.

remains unchanged (i.e., $i = f$), the transition probability amplitude is given by :

$$t_{i\to i}^{j} = \sum_{n} \frac{(\varphi_i(y)|\sqrt{\Gamma^j(y)}\,|\chi_n^j(y))(\chi_n^j(y)|\sqrt{\Gamma^j(y)}\,|\varphi_i(y))}{E - e_i^{\infty} - e_n^j}. \qquad (46)$$

For derivation of this equation see the previous section. The notation (...|...) stands for the generalized inner product which is used in non-Hermitian QM, where $(f|g) \equiv \langle f^*|g\rangle$. Note that the eigenenergies, e_n^j ,and eigenstates, $\chi_n^j(y)$, are complex due to the complex effective resonance potential. This formula can be generalized for any initial and final states by replacing $\sqrt{\Gamma^j(y)}$, which was defined in Eq.40, by the partial width amplitude of the j-th resonance state. This approach should also be used if one wants to take into account tunneling assisted by more than one resonance complex PES.

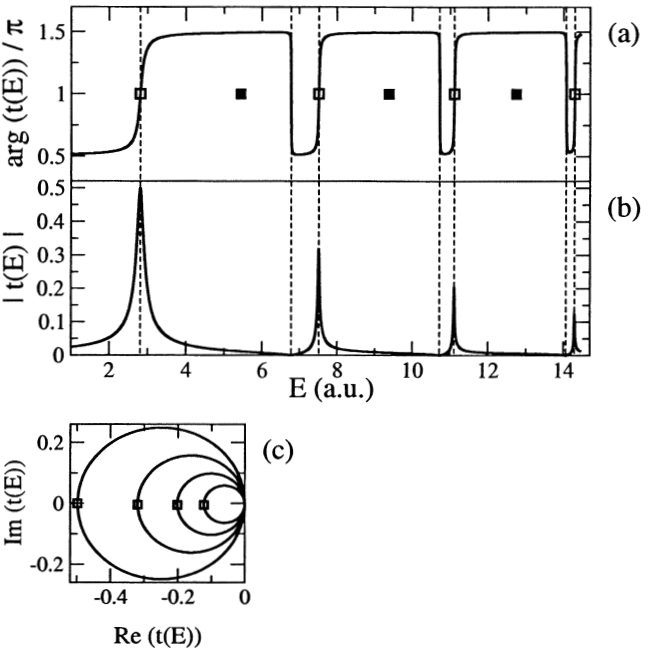

Figure 9. Transition probability amplitude, $t_{0\to 0}(E)$ assisted by the 3-rd effective complex resonance potential energy surface. (a) phase ,(b) absolute value, (c) trajectory . The phase changes by π in resonances. The phase drops by π between resonances, when $t(E)$ intersects the origin. The position of resonance states is plotted in squares (open squares - symmetric resonance states, full squares - antisymmetric resonance states). Note that due to the symmetry properties of the problem, transition is not assisted by antisymmetric resonances.

The calculated transition probability amplitude, $t^j_{0\to 0}$, is shown in Fig. 9. The transition probability shows a series of Lorentzian resonance peaks. Those appear when the energy of the incoming electron in the x direction, $E - e^{\infty}_i$, is close to the real part of the resonance energy, ϵ^j_n. Due to the symmetry of the problem, tunneling is allowed only through even resonance states.

Two distinct phenomena can be observed in Fig. 9(b), which shows the absolute value of the transition probability amplitude, as a function of the incoming electron energy, E. First, the width of the resonance peaks decreases as E increases. Second, the height of the resonance peaks decreases as E increases.

The explanation for both phenomena is based on the Breit-Wigner model for resonant tunneling. In the vicinity of a narrow isolated resonance (i.e. $\gamma_n < |\epsilon_n - \epsilon_{n\pm 1}|$), the transition probability amplitude is given

by the leading term of $t(E)$ in Eq. 46 :

$$T^j(E) \equiv |t^j(E)|^2 = \left| \frac{(\varphi_i(y)|\sqrt{\Gamma^j(y)}\,|\chi_n^j(y))}{E - e_i^\infty - e_n^j} \right|^2 \equiv \left| \frac{C_n^j}{\gamma_n^j} \right|^2 \tag{47}$$

Concerning the width of the resonance peaks, the width is associated with the inverse of the lifetime of the resonance states. The maximum of the amplitude of χ_n^j is at $y = 0$ for the first resonance state (n=0) and moves toward the classical turning points of $Re(V_{\text{eff}}^j(y))$ as n is increased (see Fig. 8). Due to the shape of the PES (see Fig. 5), the temporarily trapped electron in the QD tunnels out along the x direction mostly around $y = 0$. For higher values of $|y|$ the tunneling is hindered by the potential barriers. Therefore, the lifetime of the resonance states increases as n increases, and the corresponding widths decrease. Note that the width of the resonance peak in the transition probability graph can be associated with the inverse of the lifetime of the resonance state only if the resonances are isolated, otherwise interference phenomena between overlapping resonance states may change the Lorentzian shape of the resonance peaks.

Concerning the height of the resonance peaks, Eq. 47 shows that the height is proportional to the probability to populate the n-th resonance state. This probability is given by the overlap :

$$C_n^j \equiv |(\varphi_0(y)|\sqrt{\Gamma^j(y)}|\chi_n^j(y))|^2, \tag{48}$$

where $\varphi_0(y)$ is the initial state and $\Gamma^j(y)$ is given by the imaginary part of the resonance surface (see Eq. 46). As described above, the maximal amplitude of χ_n^j changes from $y = 0$ for the first resonance state to the classical turning points of $Re(V_{\text{eff}}^j(y))$ as n is increased. $\Gamma^j(y)$ is localized around $y = 0$, and $\varphi_0(y)$, which is the ground state of a harmonic oscillator with the frequency w_∞, gets a maximum around $y = 0$. Therefore, C_n^j decreases as n in increased. The height of the resonance peaks is also inversely proportional to the width of the resonance state, γ_n^j, which decreases as n increases. Despite of this dependence, the transition probability in resonance is dominated by the overlap and decreases as n is increased. Note that we discuss here only the resonance contribution to the transition probability amplitude and ignored the direct scattering process which dominates the high energy regime.

The phase of the transition probability amplitude, $\arg(t(E))$, changes by π when $|t(E)|$ exhibits a maximum (see Fig. 9(a)). This well-known phenomenon can be explained by the Breit-Wigner model for resonant tunneling.

The phase drops abruptly by π between resonance peaks, when the complex transition probability amplitude, $t(E)$, intersects the origin, i.e. $t(E) = 0 + i0$. This result is similar to the association of the sharp phase drop by π in the tail of the resonant peak [27, 31]. Note however that we obtained the sharp phase drop as a result of interference between two neighboring 2D resonance states which decay through the two potential barriers located at the entrance and the exit channels. This interference which leads to the sharp phase drop in $t(E)$ can not occurs in 1D double barrier potentials as we will explain below.

The energy where zero transmission is obtained is given approximately by the position of the intersection of two neighboring Lorentzian peaks (n,n+1). The position of the intersection is determined by the population of the corresponding resonance states and by their widths. On the basis of the analysis given above, the intersection is at an energy closer to the n+1 resonance peak (which is narrower and less populated that the n-th one). The energy E_0 at which $t(E_0) = 0 + i0$, can be approximately obtained by taking into account the interference between two adjacent resonance states,

$$\frac{C_n^j}{E_0 - e_i^\infty - e_n^j} + \frac{C_{n+1}^j}{E_0 - e_i^\infty - e_{n+1}^j} = 0 \quad . \tag{49}$$

Our calculations show that this approximation holds in the case presented in Fig. 9, though there is a slight deviation due to interference effects with other resonance states.

Why does the phase of $t(E)$ change abruptly by π when $t(E)$ intersects the origin ? Expanding the transition probability amplitude in a Taylor series around an intersection energy, E_0, gives :

$$t(E_0 \pm \varepsilon) = t(E_0) + \left.\frac{dt(E)}{dE}\right|_{E_0} (\pm\varepsilon) + \frac{1}{2}\left.\frac{d^2t(E)}{dE^2}\right|_{E_0} (\pm\varepsilon)^2 + \ldots \tag{50}$$

When $t(E_0) = 0$ and when ε is small enough, if $\left.\frac{dt(E)}{dE}\right|_{E_0} \neq 0$ as in our case, we get :

$$t(E_0 \pm \varepsilon) = \pm\varepsilon \left.\frac{dt(E)}{dE}\right|_{E_0} \tag{51}$$

This equality implies that in a very short energy range the phase changes by π. This is a proof that it is not necessarily true that whenever the transmission coefficient reaches zero, the phase has a sharp drop by π. The zero transmission coefficient, $t(E_0) = 0$, is a necessary condition for the sharp phase drop by π at the tail of the resonant peak but it is not a sufficient one. This abrupt phase changes happen at zero transmissions if and only if $dt(E)/dE|_{E_0} \neq 0$.

Figure 9(c) shows the trajectory of $t(E)$. At each one of the intersection energies the imaginary axis is tangent to $t(E)$ at the origin. Therefore, the first derivative of $t(E)$ is almost a pure imaginary number, and $t(E_0 \pm \varepsilon) = +i\delta$. Since in our numerical calculations $t(E)$ does not intersect the origin but passes very close to it as E is varied, the phase changes smoothly from $-\pi/2$ to $\pi/2$ instead of jumping.

The Taylor expansion of $t(E)$ shows that the transition probability does *not* jump by π when $t(E)$ intersects the origin whenever two conditions are satisfied simultaneously: (1) $t(E_0) = 0$; (2) $\frac{dt(E)}{dE}\Big|_{E_0} = 0$. In the 2D case discussed above, when $t(E)$ can be approximately obtained by taking into account only two adjacent resonance states (see Eq. 49), it is impossible to satisfy simultaneously both conditions. Therefore, whenever this approximation is valid the intersection of $t(E)$ with the origin implies a sudden change of the phase of $t(E)$ by π. Our calculations for a 1D model Hamiltonian [20] have shown that in 1D problems one can not neglect the interference of the resonances with the scattering background. Therefore, in a 1D problem it is possible to satisfy both conditions and the phase of $t(E)$ does not jump by π when $t(E)$ intersects the origin. This is another explanation for the fact that the phase drop by π at the tail of the resonant peak can *not* be obtained in a single electron transport through a double barrier 1D potential.

In this section the electron-scattering transition probability amplitude through an open QD, $t(E)$, has been studied for a real-space 2D model Hamiltonian. A sharp change of the phase of $t(E)$ by π occurs when $t(E)$ intersects the origin. It implies that two conditions should be satisfied in order to observe a sharp drop of the phase by π in the tail of the resonant peak. One condition is $t(E_0) = 0$, whereas the second condition is $dt(E)/dE|_{E_0} \neq 0$. We have shown that this phase drop is a resonance interference phenomenon that happens even within the framework of an one electron effective QD potential. The fact that the QD has at least 2D is a crucial point in the mechanism we have presented here. Our explanation of a sharp phase change is based on the destructive interference between neighboring resonances and thus differs from the mechanism based on the Fano resonance (see, for example, Refs [22, 25]).

4. Conclusions

In this work we show how the complex adiabatic approach developed within the framework of the non-hermitian quantum mechanics, enables the study of dynamics of systems which is hard and even impossible to study by the use of the conventional (hermitian) QM. We focused here on two phenomena which have been observed in two different experiments. The first one is

trapping of electrons by hydrogen molecules for time period which is by one order of magnitude longer than expected on the basis of adiabatic calculations. The second phenomena is the abrupt drop of the phase of the electrons transition probability amplitude through a 2D quantum dot. We show that both phenomena are due to the interference between overlapping resonances.

Acknowledgements

This work was supported in part by the Israel-US Binational Science Foundation, the Israeli Academy of Sciences and the Fund of promotion of research at the Technion.

References

1. E. Narevicius and N. Moiseyev, Phys. Rev. Lett. **81**, 2221 (1998).
2. E. Narevicius and N. Moiseyev, Phys. Rev. Lett. **84**, 1681 (2000).
3. U. V. Riss and H-D. Meyer J. Phys. B: At. Mol. Opt. Phys. **26**, 4503 (1993).
4. N. Moiseyev, J. Phys. B. **31**, pp. 1431-1441, 1998.
5. N. Moiseyev, Physics Reports, **302**, 211 (1998).
6. *The Lertorpet Symposium View on a Generalized Inner Product*, edited by E. Brändas and N. Elander, Lecture Notes in Physics, Vol. 325 (Springer, Berlin, 1989).
7. N. Moiseyev and S. Friedland, Phys. Rev. A. **22**, 618 (1980).
8. E. Narevicius and N. Moiseyev, J. Chem. Phys. **113**, 6088 (2000).
9. R. Santra, J. Zobeley, L.S. Cederbaum and N. Moiseyev, Phys. Rev. Lett., **85**, 4490 (2000).
10. N. Moiseyev, R. Santra, J. Zobeley and L.S. Cederbaum, J. Chem. Phys, **114**, 7351 (2001).
11. N. Moiseyev and U. Peskin, Phys. Rev. A **42**, 255 (1990).
12. L. S. Cederbaum and W. Domcke, J. Phys. B, **14**, 4665 (1981) and references therein.
13. U. Fano, Phys. Rev. **124**, 1866 (1961).
14. M. Allan, J. Phys. B, **18**, L451 (1985).
15. R. Schuster, E. Buks, M. Heiblum, D. Mahalu, V. Umansky, H. Shtrikman, Nature **385**, 417 (1997)
16. C. Mündel, M. Berman and W. Domcke, Phys. Rev. A **32**, 181 (1985).
17. N. Moiseyev and C. Corcoran, Phys. Rev. A, **20**, 814, (1979).
18. W. Domcke and L. S. Cederbaum, J. Phys. B, **13**, 2829 (1980).
19. A. Yacoby and M. Heiblum and D. Mahalu and H. Shtrikman, Phys. Rev. Lett. **74**, 4047 (1995).
20. H. Barkay and N. Moiseyev, Phys. Rev. A **64**, 44702 (2001).
21. Alessandro Silva, Yuval Oreg, and Yuval Gefen, Phys. Rev. B **66**, 195316 (2002).
22. H. Q. Xu and B. Y. Gu, J. Phys. Cond. Matt. **13**, 3599 (2001).
23. H. Q. Xu and W. D. Sheng, Phys. Rev. B **57**, 11903 (1998).
24. C. M. Ryu and S. Y. Cho, Phys. Rev. B **58**, 3572 (1998).
25. H. W. Lee, Phys. Rev. Lett **82**, 2358 (1999).
26. T. Taniguchi and M. Büttiker, Phys. Rev. B **60**, 13814 (1999).
27. P. G. Silverstov and Y. Imry, Phys. Rev. Lett **85**, 2565 (2000).
28. A. L. Yeyati and M. Büttiker, Phys. Rev. B **62**, 7307 (2000).
29. H.-W. Lee and C. S. Kim, Phys. Rev. B **63**, 075306 (2001).
30. C.-M. Ryu and S. Y. Cho, Phys. Rev. B **58**, 3572 (1998).
31. T. Chen and W. S. Liu and S. J. Xiong, Commun. Theor. Physics **35**, 121 (2001).